2009

Functional transition in the floral receptacle of the sacred lotus (Nelumbo nucifera): from thermogenesis to photosynthesis

R. E. Miller
University of Wollongong, bec@uow.edu.au

J. R. Watling
University of Adelaide, jennifer.watling@adelaide.edu.au

Sharon A. Robinson
University of Wollongong, sharonr@uow.edu.au

Functional transition in the floral receptacle of the sacred lotus (Nelumbo nucifera): from thermogenesis to photosynthesis

Abstract

The receptacle of the sacred lotus is the main source of heat during the thermogenic stage of floral development. Following anthesis, it enlarges, greens and becomes a fully functional photosynthetic organ. We investigated development of photosynthetic traits during this unusual functional transition. There were two distinct phases of pigment accumulation in receptacles. Lutein and photoprotective xanthophyll cycle pigments accumulated first with 64% and 95% of the maximum, respectively, present prior to anthesis. Lutein epoxide comprised 32% of total carotenoids in yellow receptacles, but declined with development. By contrast, more than 85% of maximum total chlorophyll, β-carotene and Rubisco were produced after anthesis, and were associated with significant increases in maximum electron transport rates (ETR) and photochemical efficiency (Fv/Fm). Leaves and mature receptacles had similar Rubisco content and ETRs (>200 μmol m-2 s-1), although total chlorophyll and total carotenoid contents of leaves were significantly higher than those of green receptacles. Receptacle δ13C prior to anthesis was similar to that of leaves; consistent with leaf photosynthesis being the source of C for these tissues. In contrast, mature receptacles had significantly lower δ13C than leaves, suggesting that 14-24% of C in mature receptacles is the result of refixation of respired CO2.

Keywords

photosynthesis, greening, Rubisco, development, chlorophyll, violaxanthin, antheraxanthin, zeaxanthin, ß-carotene, lutein epoxide

Disciplines

Life Sciences | Physical Sciences and Mathematics | Social and Behavioral Sciences

Publication Details

This article was originally published as Miller, RE, Watling, J and Robinson, SA, Transitioning from heater to seed production – the photosynthetic stage of the sacred lotus (Nelumbo nucifera) receptacle, Functional Plant Biology, 36(5), 2009, 471-480. Original article available here.

Title

Functional transition in the floral receptacle of the sacred lotus (*Nelumbo nucifera*): from thermogenesis to photosynthesis

Running head

Photosynthesis in the sacred lotus receptacle

Authors

Rebecca E Miller[ab*]
Jennifer R Watling[a]
Sharon A Robinson[b]

[a]School of Earth and Environmental Sciences, University of Adelaide, Adelaide, South Australia 5005, Australia. Email: jennifer.watling@adelaide.edu.au

[b]Institute for Conservation Biology, Department of Biological Sciences, University of Wollongong, Wollongong, New South Wales 2522, Australia. Email: sharonr@uow.edu.au

*corresponding author, current address: School of Biological Sciences, Monash University, Victoria 3800, Australia. Email: rebecca.miller@sci.monash.edu.au

Keywords (5-8) photosynthesis, greening, Rubisco, development, chlorophyll, violaxanthin, antheraxanthin, zeaxanthin, ß-carotene, lutein epoxide

Abstract

The receptacle of the sacred lotus is the main source of heat during the thermogenic stage of floral development. Following anthesis, it enlarges, greens and becomes a fully functional photosynthetic organ. We investigated development of photosynthetic traits during this unusual functional transition. There were two distinct phases of pigment accumulation in receptacles. Lutein and photoprotective xanthophyll cycle pigments accumulated first with 64% and 95% of the maximum, respectively, present prior to anthesis. Lutein epoxide comprised 32% of total carotenoids in yellow receptacles, but declined with development. By contrast, more than 85% of maximum total chlorophyll, β-carotene and Rubisco were produced after anthesis, and were associated with significant increases in maximum electron transport rates (ETR) and photochemical efficiency (F_v/F_m). Leaves and mature receptacles had similar Rubisco content and ETRs (>200 μmol m^{-2} s^{-1}), although total chlorophyll and total carotenoid contents of leaves were significantly higher than those of green receptacles. Receptacle $\delta^{13}C$ prior to anthesis was similar to that of leaves; consistent with leaf photosynthesis being the source of C for these tissues. In contrast, mature receptacles had significantly lower $\delta^{13}C$ than leaves, suggesting that 14-24% of C in mature receptacles is the result of refixation of respired CO_2.

Introduction

In many species, growth of fruit does not only depend on plant carbohydrate reserves and foliar CO_2 assimilation, but also on photosynthesis in reproductive tissues. Photosynthetic activity – both during anthesis and subsequent fruit development – has been identified in reproductive structures of a range of species; including the anthers of *Lilium* (Clément *et al.* 1997) and *Triticum aestivum* (Kirichenko *et al.* 1993), sepals of *Helleborus niger* (Salopek-Sondi *et al.* 2000), sepals and receptacle of apple (Vemmos and Goldwin 1994), as well as embryos of several species (e.g. *Brassica napus*; Eastmond and Rawsthorne 1998). Non-foliar photosynthetic rates vary widely, not only with reproductive structure, but also with developmental stage. The overall contribution of this reproductive CO_2 assimilation also varies widely among species and can be substantial. Among 15 temperate deciduous trees, the contribution of flower and fruit photosynthesis to C required for the production of mature seed ranged from 2.3% to 64.5% (Bazzaz *et al.* 1979). Photosynthesis in barley ears

contributes up to 13% of final grain weight (Biscoe *et al.* 1975), photosynthetic activity of reproductive tissues of apple contributes 15-33% of flower and fruit carbohydrate requirement (Vemmos and Goldwin 1994) and similarly, 38% of C incorporated by seeds of *Pisum sativum* (pea) is derived from pod photosynthesis (Flinn and Pate 1970).

In addition to direct fixation of atmospheric CO_2, reproductive tissues of many species also contribute to overall C balance via the recycling of respired CO_2 (Harvey *et al.* 1976). In particular, refixation of respired CO_2 has been reported in the pods of legumes and other seed bearing structures which reassimilate CO_2 respired by the enclosed seed (e.g. *Cicer arietinum* (chickpea); Furbank *et al.* 2004). The extent of refixation differs among species. For example, respired CO_2 was the main source for glume photosynthesis in wheat (*Triticum aestivum*), constituting 73% of CO_2 fixed by the ear (Gebbing and Schnyder 2001). By contrast, in cotton, recycled CO_2 contributed around 10% of total C for fruit growth (Wullschleger *et al.* 1991). Interestingly, in some chlorophyllous reproductive tissues energy from light absorption is not only used for CO_2 assimilation, but also for other processes. In *Brassica napus* (oilseed rape), for example, light activation of photosynthetic enzymes in seeds is important not only for refixation of respired CO_2 by Rubisco, but also for fatty acid synthesis (Ruuska *et al.* 2004).

Here, we investigate photosynthetic activity in the floral receptacle of the aquatic perennial sacred lotus (*Nelumbo nucifera* Gaertn.) which may similarly contribute to carbohydrate balance and metabolic processes during seed maturation. Unusually, the receptacle of this species transitions from a highly active respiratory organ, able to heat to more than 20˚C above ambient, to a large photosynthetic, seed-bearing structure. This prominent receptacle is yellow during the early stages of floral development, including during stigma receptivity. Following anthesis and cessation of thermogenesis the receptacle enlarges and greens, becoming photosynthetic (over a 2-4 day period; Watling *et al.* 2006; Grant *et al.* 2008). In this paper we report on the changes associated with this unusual functional transition from a thermogenic to a photosynthetic organ during flower and fruit development. Specifically, we measured changes in photosynthetic rate, Rubisco content, and photosynthetic and photoprotective pigments throughout receptacle development, compared photosynthetic characteristics of green receptacles and leaves, and investigated the potential for recycling of respired CO_2 by the receptacle.

Materials and Methods

Sampling

Nelumbo nucifera (Gaertn.) flowers were sampled from a population in the Adelaide Botanic Gardens, South Australia during the 2005-2006 and 2006-2007 summer seasons. Flowers were categorised into six distinct developmental stages following Grant *et al.* (2008). These stages are: developing bud enclosing a small yellow receptacle (stage 0), mature bud enclosing a small yellow receptacle (stage 1), petals open 2-12 cm, immature stamens appressed to yellow receptacle (stage 2), petals horizontal revealing mature stamens, onset of greening (stage 3), petals and stamens abscised leaving a small, yellow-green receptacle (stage 4), and enlarged green receptacle (stage 5) (Supplementary Fig. 1). Flowers from each developmental stage were sampled (n=5-8). The stem was cut at least 20 cm below the flower, recut under water and transported back to the lab in a bottle of pond water. The time between cutting flowers and making measurements in the lab did not exceed 20 min. Light response curves were measured by chlorophyll fluorescence (see below) in the laboratory, following which the top pigmented tissue layer (approx. 1 mm thickness; Supplementary Fig. 2) of the receptacle was excised, frozen in liquid N_2 and stored at -80ºC for later analysis of Rubisco and pigments, as described below.

Light response curves

Light response curves of chlorophyll *a* fluorescence parameters were measured in the lab on detached receptacles (stages 3, 4 and 5; n=6-8), and on leaves in the field using a mini-PAM fluorometer (Walz, Effeltrich, Germany). Leaves and receptacles were first dark adapted for 30 min and maximum quantum yield of photosystem II (PSII) was determined as the ratio of variable to maximum fluorescence (Fv/Fm) (Maxwell and Johnson 2000). Samples were then subjected to a moderate PFD (360 μmol m^{-2} s^{-1}) until steady state fluorescence was attained. After induction, light response curves were obtained using the mini-PAM light-curve program, where PFD was increased across 8 points from 0 to 1500 μmol m^{-2} s^{-1} over 3 minutes. The effective quantum yield of ΦPSII [= quantum efficiency of PSII; (Fm′-F)/Fm′], and non-photochemical quenching [NPQ=(Fm-Fm′)/Fm′] were calculated, where F is the steady-state fluorescence yield and Fm′ is the maximum fluorescence yield, of the illuminated sample. The apparent rate of photosynthetic electron transport of PSII (ETR) was determined from the equation ETR= ΦPSII x PFD x 0.5 x 0.84 (Maxwell and Johnson 2000). Several (3-4) light response curves measured at different locations on the surface of each receptacle and

leaf were averaged. An exponential curve [f=a*(1-exp(-b*x)] was fitted to the mean ETR response curve using Sigmaplot 9.0 (SPSS Inc) from which the maximum photosynthetic electron transport rate (ETR_{sat}) and saturating PFD (PFD_{sat}) were determined for each sample. In addition, instantaneous in situ measurements of apparent ETR of leaves and receptacles of different stages were taken in the field on a clear afternoon (incident PFD approx. 1350 μmol m^{-2} s^{-1}).

Rubisco determination

Extraction

Proteins were extracted from receptacles in stages 1-5. Frozen samples (~0.25 g FW) of the upper surface (1 mm thick) of the receptacle were finely ground in liquid N_2, and homogenised in cold acetone with 10% (w/v) TCA, 0.07% v/v β-mercaptoethanol and 1% (w/v) PVPP (4:1 v/w, acetone:tissue) as described by Santoni *et al.* (1994). Proteins were allowed to precipitate overnight at -20ºC. Samples were centrifuged (15 min, 16000 *g* at 4ºC), and the pellet was twice washed in acetone with 0.07% β-mercaptoethanol, incubated at -20ºC for 30 min each time and centrifuged (15 min, 16000 *g* at 4ºC). The pellet was then air dried and resuspended in protein solubilisation buffer [62 mM Tris, 65 mM DTT, 10% (v/v) glycerol, 2% (w/v) SDS pH 6.8]. Following centrifugation, the proteins in the supernatant were precipitated by the addition of cold acetone with 0.07% β-mercaptoethanol for 5 h at -20ºC. After centrifugation (15 min, 16000 *g* at 4ºC), the precipitate was air dried, and resuspended in 100 μL of the same solubilisation buffer. The protein concentration was determined using the RCDC detergent compatible BioRad protein kit (BioRad).

Electrophoresis and western blotting

Proteins were separated by SDS-PAGE using a Bio-Rad mini protean II electrophoresis system (Bio-Rad) with the (Laemmli 1970) buffer system. Equal amounts of total protein were loaded onto a 12% polyacrylamide resolving gel with 4% stacking gel. Proteins were transferred to polyvinylidene fluoride (PVDF) membrane (Millipore Immobilon 0.45 μm) using a method similar to Harlow and Lane (1988). Following transfer, membranes were blocked with 5% skim milk/Tris-buffered saline with Tween [TBST; 20 mM Tris, 140 mM NaCl, 1% (v/v) Tween-20] for 2 h, and incubated overnight at 4ºC in primary antibody raised to spinach Rubisco (holoenzyme) (1:5000 in 5% milk/TBST) (Whitney and Andrews 2001). Membranes were washed 3 times in TBST and then probed with the secondary antibody [goat

anti-rabbit HRP conjugate (Pierce; 1:4000 in 5% milk/TBST)] for 1 h. Immunoreactive protein bands were visualised using SuperSignal West Femto Maximum Sensitivity Substrate (Pierce) by a Fluorchem 8900 Gel Imager and analysed using Fluorchem IS-8900 software (Alpha Innotech, San Leandro, CA). A serial dilution was carried out to ensure there was a linear relationship between protein loaded and densitometry; Rubisco quantitation by chemiluminescence was linear within the range of concentrations detected, and is expressed as chemiluminescence output per g protein loaded per gel lane.

Carbon Isotope Analysis

The carbon isotope composition of receptacles and leaves was determined using oven dried (70ºC), and ground, leaf and stage 3, 4 and 5 receptacle samples (n=5). The relative abundance of ^{13}C and ^{12}C isotopes in the CO_2 produced from combustion of these samples was analysed using a Tracermass Ion Ratio Mass Spectrometer and Roboprep preparation system (Europa PDZ, UK now Sercon Pty Ltd), calibrated using atropine and acetanilide (Microanalysis Ltd., UK). Isotopic composition is expressed as $\delta^{13}C$ per mil (δ ‰) relative to the VPDB (Vienna Pee Dee Belemnitella) standard.

Pigment extraction and quantification

Pigments in the top tissue layers of frozen (-80ºC) receptacles (~0.1-0.15 g FW) and leaves (0.1 g FW) were extracted with sequential cold acetone extractions (100%, 80%, 80%, 80%) as described in Dunn *et al.* (2004), but with an additional extraction in 80% acetone. The extracts were analysed by HPLC using the method of Dunn *et al*. (2004) adapted from Gilmore and Yamamoto (1991). Pigments were separated on a SphereClone 5µm ODS1 column (250 x 4.6 mm: Phenomenex, Sydney, NSW). Solvent A was varied to be MeCN:hexane:Tris-HCl 0.1M pH 8.0 (83:11:6), while solvent B was unchanged (MeOH:hexane, 4:1). Pigment concentrations were calculated using co-efficients determined from pigment standards. For unknown carotenoids, the co-efficient for β-carotene was used. In order to best compare green receptacles with leaves, concentrations of pigments (g^{-1} FW) in stage 5 receptacles were converted to concentrations per unit area using the relationship between surface area and tissue FW of the excised pigmented tops (1 mm thick) of receptacles.

Statistical Analyses

Data were analysed using JMP 5.1 (SAS Institute Inc.). Data were tested for normality using the Shapiro-Wilk W Test. Levene's test was applied to ensure homogeneity of variances. Fluorescence data satisfied normality and homogeneity of variance and were analysed by 1 way ANOVA, and the Tukey HSD post-hoc test was used to identify differences at $P<0.05$. Total chlorophyll, neoxanthin, lutein and VAZ were square root transformed and Rubisco and β-carotene data were log transformed to satisfy the assumptions of ANOVA. T tests were used to compare stage 5 and leaf pigment concentrations per unit area.

Results

Rubisco was present in receptacles of stages 1-5, but increased significantly throughout development ($P<0.0001$; Fig. 1a). Rubisco content of stage 1-3 receptacles was similar, but there was a significant doubling from stage 1 to stage 4. The largest increase was between stage 4 and 5 when Rubisco content more than trebled (Fig. 1a). Overall, 85% of Rubisco was produced after thermogenesis had ceased, following abscission of the petals and stamens (i.e. after stage 3). No significant difference in Rubisco content of leaves and stage 5 receptacles was detected ($P=0.35$; Fig. 1a).

The accumulation of chlorophyll during receptacle development was similar to that of Rubisco (Fig. 2b). Total chlorophyll (*a+b)* concentration per unit mass was very low in stage 0 to 2 receptacles but increased 4-fold from stage 3 to stage 4 ($P<0.0001$), and then more than doubled to 421.6 ± 25.5 nmol g^{-1} FW in mature, green stage 5 receptacles (Fig. 2b). In contrast to Rubisco, which did not differ on a total protein basis between leaves and stage 5 receptacles (Fig. 1a), total chlorophyll (*a+b*) was significantly higher in leaves than stage 5 receptacles ($t_{4.1}=-13.2$, $P<0.0001$). This was also the case when the comparison was made on an area basis, with leaves having 70% higher chlorophyll content than stage 5 receptacles ($t_{6.5}=-5.4$, $P=0.0006$; data not shown).

Total carotenoids also increased significantly throughout development ($P<0.0001$); however, in contrast with chlorophyll, 83% of the maximum total carotenoids present in stage 5 receptacles had accumulated by stage 2 (Fig. 1c). The pattern of accumulation of total carotenoids was largely driven by changes in the most abundant carotenoid, lutein, and in the xanthophyll cycle (VAZ) pigments (Fig. 2a-b). β-carotene ($P<0.0001$), and neoxanthin ($P<0.0001$) also increased significantly throughout development (Fig. 2c-d). In contrast with

total chlorophyll and β-carotene which increased dramatically at stages 4 and 5, respectively (Fig. 1b, 2d), 95% of the maximum VAZ pool, 64% of maximum lutein and 50% of neoxanthin had accumulated in yellow receptacles by stage 2 (Fig. 2a,c). Lutein epoxide was the only carotenoid to decrease during development, declining from 8.76 ± 0.41 nmol g^{-1} FW at stage 0 to 1.79 ± 0.20 nmol g^{-1} FW at stage 5 (P<0.0001; Fig. 2a). Across all stages, the VAZ pool constituted approximately a third (mean 34.6%) of the total carotenoid pool in receptacles, a proportion which changed little during development (Table 1). By contrast, lutein and β-carotene increased as a proportion of total carotenoids during receptacle development, while the proportion of lutein epoxide decreased. In stage 0 receptacles, lutein epoxide constituted 32.3% of the total carotenoid pool, this proportion declining to 1.8% in stage 5 receptacles (Table 1).

The carotenoid composition of stage 5 receptacles and leaves differed significantly (Fig. 1c, Table 1). The proportions of lutein ($t_{4.2}$=-3.15, P=0.032) and neoxanthin ($t_{6.2}$=-4.6, P=0.003) were significantly higher in leaves than green receptacles. In contrast, the proportions of VAZ ($t_{4.7}$=3.54, P=0.018) and lutein epoxide ($t_{9.4}$=3.4, P=0.0037) were significantly higher in receptacles than leaves. VAZ content relative to total chlorophyll (VAZ/Tchl) was also higher in stage 5 receptacles than leaves, with concentrations of 0.08±0.01 and 0.04±0.01 mol mol^{-1} Tchl, respectively ($t_{9.9}$=3.98, P=0.0027). The ratio of chlorophyll *a*:*b* did not change throughout development or between leaves and green receptacles (P=0.22; data not shown).

Associated with the significant increases in total chlorophyll, Rubisco and total carotenoids across stages 3-5, was a significant increase in photosynthetic capacity ($F_{2,21}$=47.4, P<0.0001; Fig. 3; Table 2). Following petal and stamen abscission, maximum ETR (ETR_{sat}) increased significantly with each developmental stage, increasing 3-fold from 41.5 ± 6.2 μmol m^{-2} s^{-1} at stage 3 to 128.8 ± 6.5 μmol m^{-2} s^{-1} at stage 5 (Fig. 3). The PFD at which electron transport saturated almost doubled from 700 μmol m^{-2} s^{-1} to more than 1300 μmol m^{-2} s^{-1} between stages 3 and 4 (Fig. 3). Light response curves of stage 5 receptacles measured in the lab and in the field indicated that electron transport was not fully saturated at a PFD of 1500 μmol m^{-2} s^{-1}. Since we were unable to measure light response curves of leaves in the lab, due to excessive wilting, we also performed instantaneous measurements of ETR on receptacles and leaves in the field to enable direct comparison of ETRs of leaves and receptacles. On a sunny day under similar incident PFD (1350 μmol m^{-2} s^{-1}) ETRs of stage 5 receptacles and leaves were not

significantly different at 201.6 ± 5.5 and 208.3 ± 8.7 μmol m^{-2} s^{-1}, respectively (Table 2). Under the same conditions, the mean ETR of stage 4 receptacles (158.5± 8.8 μmol m^{-2} s^{-1}) and stage 3 receptacles (92.5± 6.0 μmol m^{-2} s^{-1}) was significantly lower than leaf and stage 5 receptacle rates, but notably higher than ETR_{sat} determined from light response curves measured in the lab (Table 2; Fig. 3). However as was found in the lab measurements there was a significant increase in ETR_{sat} at each stage, with stages 3 and 4 receptacles achieving 45% and 79% of the maximum rate achieved in stage 5 receptacles.

The maximum photochemical efficiency (Fv/Fm) also increased significantly with greening (Table 2) and the effective quantum yield of receptacles of all stages decreased with rising PFD (Fig. 3). Stage 3 receptacles, which had the lowest intrinsic quantum yields (Fv/Fm; Table 2), also showed the greatest decline (83%) in effective quantum yield (ΦPSII) with increasing PFD (Fig. 3). Conversely, stage 5 receptacles, had the lowest relative decline in ΦPSII with increasing PFD. No photochemical activity was detected by fluorometry in prethermogenic buds (stage 0) which had negligible chlorophyll (Fig. 1b), or in stage 1 or 2 receptacles, which had low chlorophyll and Rubisco content (Fig. 1a-b). Non-photochemical quenching (NPQ) was highly variable in stage 3 receptacles but tended to be higher than in stage 4 and 5 receptacles, particularly at lower PFDs (Fig. 3c). NPQ in stage 3 receptacles was significantly higher than in stage 5 receptacles at PFDs up to 160 μmol m^{-2} s^{-1} ($F_{2,16}$=4.15, P=0.0385), but did not differ significantly between developmental stages at higher PFDs (Fig. 3c).

Yellow stage 3 receptacles and leaves had similar $\delta^{13}C$ values (Table 3), suggesting a shared C source. As the receptacle greened, however, $\delta^{13}C$ became gradually more negative suggesting a shift to independent C fixation by stage 4 and 5 receptacles ($F_{3,19}$=17.7, P<0.0001). By stage 5, $\delta^{13}C$ was significantly lower than in both earlier stage receptacles, and leaves (Table 3).

Discussion

Pigment composition in yellow and green receptacles

Consistent with the change in function of the receptacle, from a yellow thermogenic structure involved in pollinator attraction, to an enlarged photosynthetic structure that probably

supports seed maturation, we observed two phases in pigment accumulation during development. In the early stages, prior to anthesis, lutein, lutein epoxide (Lx), xanthophyll cycle pigments (VAZ), and to a lesser extent neoxanthin accumulated (Fig. 2). At stage 2, when the flower first fully opened to reveal receptive stigma, lutein, Lx and VAZ together comprised 81% of the total carotenoid pool. In addition, a high proportion of other unidentified carotenoids (11%; Table 1) was also found at stage 2. This pigment composition is responsible for the strong yellow colour of the receptacle, a colour known to be attractive to insect pollinators (Kevan 1983), and which together with enhanced scent volatilisation by thermogenesis (Meeuse 1975), presumably plays an important role in drawing pollinators to receptive stigmas. At this stage in floral development, these carotenoids may also function in photoprotection, their antioxidant properties limiting damage by reactive oxygen species (ROS) to light-sensitive membranes and enzymes during chloroplast maturation (Robinson and Russell 1999; Merzlyak and Solovchenko 2002).

During the second phase, following anthesis and abscission of stamens and petals late in stage 3, carotenoid concentrations again increased, with the biggest proportional increases in neoxanthin and β-carotene (Fig. 2). In addition, there were large compositional changes from stage 3-5 in plastid pigment composition, driven by the massive increase in total chlorophyll (Fig. 1). Although β-carotene is the biosynthetic precursor for a number of other carotenoids (e.g. VAZ, neoxanthin) it comprised only a small proportion of total carotenoids during anthesis (1.5% at stage 2), but was the only pigment to accumulate more or less proportionally with total chlorophyll across all developmental stages (Fig. 2d), a pattern closely mirrored by the accumulation of Rubisco (Fig. 1). The dip in concentrations of most pigments between the two phases (at stage 3; Fig. 1c, 2) most likely reflects changes in plastids during this functional shift at the end of anthesis and onset of greening. Plastid characteristics during this transition have not been described in lotus, thus it is not known whether the transition involves only the transformation of existing chromoplasts, or whether *de novo* formation of plastids occurs.

Lutein epoxide – a derivative of the α-carotene branch of the carotenoid biosynthetic pathway by epoxidation of lutein (García-Plazaola *et al.* 2007) – was the only carotenoid to decrease during receptacle development (Fig. 2a). In young yellow receptacles Lx accounted for 32.3% of the total carotenoid pool, and resulted in a high mean Lx/VAZ ratio of 0.96. By stage 5, Lx

comprised on average only 1.6% total carotenoids and Lx/VAZ had declined to 0.05 (Fig. 2a; Table 1). Lutein epoxide has a limited taxonomic distribution, found in only 58% of 50 families analysed prior to the review of García-Plazaola *et al*. (2007). The relative abundance of Lx in early stages of lotus receptacle development is high when compared with reports for chromoplasts of other non-foliar tissues including fruits (e.g. grape; Razungles *et al.* 1996), flowers (e.g. daylily; Tai and Chen 2000) and seeds (e.g. pumpkin; Matus *et al.* 1993) where it occurs only in low concentrations and comprises no more than 5% of total carotenoids.

In contrast the concentrations of Lx relative to total chlorophyll in mature green receptacles and lotus leaves – 3.7 and 0.93 mmol mol^{-1} Tchl, respectively – fall within the wide range of values reported for photosynthetic tissues of other species. Foliar Lx concentrations range from around 1 mmol Lx mol^{-1} Tchl in a many species (García-Plazaola *et al.* 2007), up to 78 mmol Lx mol^{-1} Tchl in shade leaves of *Inga* spp. (Matsubara *et al.* 2005). Higher foliar concentrations (> 20 mmol Lx mol^{-1} Tchl) are restricted to relatively few taxa in the Fagaceae, Lauraceae and Fabaceae families, and to photosynthetic stems of parasitic *Cuscuta* and *Cassytha* spp. (García-Plazaola *et al.* 2007). The few documented Lx concentrations in photosynthetic reproductive tissues are higher than for green lotus receptacles. In green peas, Lx content ranged from 9.4-12.8 mmol Lx mol^{-1} Tchl, and comprised 4-5% total carotenoids (Edelenbos *et al.* 2001), while in the pericarp of mature green tomatoes this proportion was 19%, and 8 mmol Lx mol^{-1} Tchl was found (Rabinowitch *et al.* 1975).

The Lx cycle is hypothesised to provide protection against excess light in shade leaves via sustained energy dissipation and the reversible down regulation of photosynthesis (Matsubara *et al.* 2007; Esteban *et al.* 2008). Because the same enzyme, VDE (violaxanthin de-epoxidase), which catalyses the de-epoxidation of violaxanthin to zeaxanthin also catalyses the conversion of Lx to lutein (Bungard *et al.* 1999), the Lx cycle can potentially function in all species (García-Plazaola *et al.* 2003). The operation of the full cycle however, has only been demonstrated in a few species to date (García-Plazaola *et al.* 2002; Watson *et al.* 2004; Close *et al.* 2006; Esteban *et al.* 2008) and its operation appears to be highly species dependent (Esteban *et al.* 2007). The pericarp of mature green tomato is the only fruit tissue in which Lx cycle activity has been demonstrated (Rabinowitch *et al.* 1975).

The substantial amounts of Lx in yellow lotus receptacles suggest Lx is important during early stages of floral development, however the interconversion of Lx and lutein was not

specifically investigated in this study, and indeed, Lx-cycle function in chromoplasts of non-photosynthetic tissues remains to be demonstrated (García-Plazaola *et al.* 2003; García-Plazaola *et al.* 2004). During stage 0 and 1, when the receptacle is enclosed within the bud, it seems unlikely that there would be diurnal Lx-cycle activity to provide photoprotection. While Lx declined rapidly as a proportion of total carotenoids from stage 1 (Table 1), actual Lx concentrations only decreased from stages 3 to 5 when the receptacle was first exposed to full sun during the second phase of pigment accumulation associated with greening. Similar ontogenetic variation has been found in chlorophyllous tissues; Lx accumulates in the shaded inner leaf primordia in buds of woody species, where upon budburst it is irreversibly photoconverted to lutein (García-Plazaola *et al.* 2004). Thus during the chromoplast-chloroplast transition, the Lx-cycle in lotus receptacles may be analogous to the 1-way truncated Lx-cycle in shaded buds upon budburst, when additional lutein synthesis may be important for stabilisation of new light harvesting complexes (García-Plazaola *et al.* 2007), and when, in conjunction with the xanthophyll cycle activity, de-epoxidation of Lx may provide an additional means of photoprotective energy dissipation upon first exposure to full sunlight (Matsubara *et al.* 2005; Matsubara *et al.* 2007).

In receptacles in the early stages of greening, where light absorption may quickly exceed photosynthetic capacity, there was evidence of a greater reliance on mechanisms of photoprotective energy dissipation. Stage 3 receptacles, which had significantly higher VAZ/Tchl ratios than stage 4 and 5 receptacles, also had significantly higher NPQ than stage 5 receptacles, particularly at lower irradiances (Fig. 3c). The lag in increasing NPQ with PFD in stage 5 receptacles is consistent with their greater photochemical capacity and therefore lesser requirement for NPQ under low irradiance (Fig. 3c).

Photosynthetic activity in green receptacles and leaves

Green lotus receptacles contain the full complement of higher plant photosynthetic pigments, on the whole in similar proportions to lotus leaves and to other species (Thayer and Björkman 1990; Peng *et al.* 2006). The mean and maximum Tchl concentrations of green receptacles were within the range measured in other fruits - higher than the concentrations in peel of *Malus* (apple), tomato pericarp, and Capsicum, but lower than in *Cucurbita* (pumpkin) peel (Smillie *et al.* 1999; Aschan and Pfanz 2003). The Tchl concentrations per unit area in lotus receptacles were 60% of Tchl concentrations in lotus leaves. Interestingly, it is not unusual for green reproductive structures to have equivalent or higher photosynthetic rates on a per

chlorophyll basis than leaves of the same species (Blanke and Lenz 1989; Wullschleger *et al.* 1991; Aschan and Pfanz 2003).

The high ETR of stage 5 receptacles was comparable both with lotus leaves under moderately high PFD (1350 μmol m^{-2} s^{-1}) and with leaves from other species (Aschan *et al.* 2005). Although a similarly high ETR of 203 μmol m^{-2} s^{-1} was reported for the green stage of tomato pericarp at a PFD of 1200 μmol m^{-2} s^{-1} (Smillie *et al.* 1999) these high ETRs are substantially greater than those reported for a range of other reproductive structures (e.g. Aschan and Pfanz 2003; Aschan *et al*. 2005). Lotus is also unusual since most species show lower ETRs of photosynthetic reproductive tissues than leaves (Aschan and Pfanz 2003). The maximum ETRs of fruit and persistent sepals of *Helleborus,* for example, were 80% of leaf ETRs (Aschan *et al.* 2005).

Based on fluorescence data, it is difficult to draw conclusions about comparative CO_2 fixation rates of lotus receptacles. In some fruits, high ETRs do not result in substantial CO_2 fixation, suggesting that light capture and electron transport may be used for other processes (Aschan and Pfanz 2003). Embyros of *Brassica napus*, for example, harvest light but do not necessarily assimilate CO_2, energy from light reactions is instead used for fatty acid synthesis (Asokanthan *et al.* 1997; Ruuska *et al.* 2004). Consequently, the comparable ETRs of lotus leaves and receptacles do not necessarily mean equivalent CO_2 fixation rates, nor that the receptacle performs net CO_2 fixation. The high Rubisco content in sacred lotus receptacles does however suggest that this organ is primarily involved in CO_2 fixation via the C3 pathway. Whether the receptacles have similar rates of atmospheric CO_2 fixation as leaves, will also depend on the availability of CO_2. Fruiting structures and leaves in other species often have lower stomatal density than leaves (Aschan and Pfanz 2003). While capacity for net fixation of atmospheric CO_2 by fruit varies during development and with tissue type, non-foliar photosynthetic tissues are also capable of recycling of seed-derived respired CO_2 (Goldstein *et al*. 1991; Gebbing and Schnyder 2001). As in legume pods, where the exocarp fixes exogenous CO_2 and the endocarp fixes CO_2 released from seed respiration (Goldstein *et al.* 1991), photosynthesis in the outer pigmented layers of the receptacle may similarly draw upon both atmospheric CO_2 and CO_2 derived from respiration (Supplementary Fig. 2).

Source CO_2 - potential refixation of respired CO_2

Leaf and receptacle $\delta^{13}C$ values were within the range for C3 plants. The C isotope composition of stage 3 receptacles and leaves was similar (Table 3) indicating that stage 3 receptacles, prior to substantial greening, are composed primarily of C derived from fixation of atmospheric CO_2 by leaves. There are a number of possible explanations for the subsequent significant decline in $\delta^{13}C$ (by 2.16‰) following anthesis (Table 3). It could result from changes in the ratio of internal:external CO_2 (Ci/Ca). Increases in Ci/Ca, as a result of low PFD or increased water availability, can lead to similar declines in $\delta^{13}C$ (Lüttge *et al.* 2001). In this study however, environmental conditions were unchanged throughout development. In addition, if stage 5 receptacles did have similar rates of photosynthesis as leaves, as is suggested by the similar ETRs and Rubisco contents, it is more likely that Ci/Ca ratios would be lower because of the low stomatal density. This would result in higher $\delta^{13}C$ in stage 5 receptacles than in leaves, rather than the lower values observed.

The decline could also result from variation in the $\delta^{13}C$ of source air. That is, as the receptacle ages, some C may derive from the refixation of respired CO_2, which is already depleted in ^{13}C, and which would result in a lower tissue $\delta^{13}C$ than C sourced solely from atmospheric CO_2. The decline by 2.16‰ is similar to those found within forest canopies (of 2-5‰; e.g. Buchmann *et al.* 1997; Kondo *et al.* 2005), where the lower $\delta^{13}C$ values closer to the ground are attributed in part to greater refixation of respired CO_2 (Griffiths 1993; Heaton and Crossley 1995; Sternberg *et al.* 1997; Kondo *et al.* 2005). A substantial part of this respired CO_2 could derive from the under water rhizomes which vent air via the stems. This would supplement atmospheric CO_2 supply, which could be limited by the low stomatal density of receptacles. In fact, it is difficult to see how stage 5 receptacles could have sustained similar ETRs to those of leaves without an extra source of CO_2. The high Rubisco content and ETR light response curves of the green stage 5 receptacles suggest C3 pathway activity in stage 5 receptacles. Thus, while PEP carboxylase is involved in C fixation in fruit of some C3 plants (e.g. apple; Blanke *et al.* 1986), it seems unlikely that PEPc is contributing significantly to photosynthetic C fixation in lotus.

If we assume that all C fixation in receptacles occurs via the C3 pathway (i.e. Rubisco only), we can estimate the proportion of respired CO_2 fixed by green receptacles by comparing the observed $\delta^{13}C$ with that expected if there was 100% respiratory CO_2 fixation. Using the C3 discrimination value (Δ) of 20.1‰ (Farquhar *et al.* 1989), and a source $\delta^{13}C$ of -25.24‰ (i.e. the signature of leaf tissue) we would expect a receptacle $\delta^{13}C$ of -44.5 or -42.5‰ allowing

for either no fractionation (Lin and Ehleringer 1997) or some fractionation during respiration (^{13}C enrichment by 2‰; (Duranceau *et al.* 2001). Based on the comparison of the expected $\delta^{13}C$ with the observed $\delta^{13}C$ in stage 5 receptacles, 14-24% of fixed C is derived from respiratory CO_2 in stage 5 receptacles.

While this proportion is similar to the proportion of respired CO_2 refixed by canopies in which similar declines in $\delta^{13}C$ are reported (e.g. Schleser 1990; Kondo *et al.* 2005), it is difficult to compare this value with reproductive tissues of other species as the proportion of respired CO_2 that is recycled is more commonly reported than its relative contribution to total fixed C. This range (14-24%) however, is substantially less than estimates for other species, in which the seed is more tightly enclosed within a pod or other photosynthetic structures, allowing for relative accumulation of respired CO_2 which consequently comprises a greater proportion of C fixed. In the wheat ear, for example, where grains are tightly enclosed within the glume, respiratory CO_2 was the main source for glume photosynthesis contributing 73% of CO_2 to sucrose accumulation (Gebbing and Schnyder 2001). Similarly high proportions have been found for pods of legumes (e.g. Furbank *et al*. 2004). Unlike legumes and cereals, lotus receptacles are open to the atmosphere (Supplementary Fig. 2), enabling greater mixing of respired and atmospheric CO_2. Thus the lower relative contribution of recycled CO_2 is not surprising.

The lotus receptacle is yellow during anthesis, green during fruit development, and brown at seed maturation when the receptacle inverts and falls, forming a buoyant dispersal agent for seeds. Receptacle coloration during seed maturation is therefore not to aid seed dispersal by an animal vector in this species. Instead, the receptacle is among green ripe fruits for which the capacity for photosynthesis could be considered the main ecological advantage (Cipollini and Levey 1991). Photosynthesis in the seed bearing receptacle of lotus is an effective strategy for reducing the costs of reproduction (Aschan and Pfanz 2003), by both the direct assimilation of atmospheric CO_2 (e.g. wheat, tomato, cotton, pea) and through the recycling of respired CO_2 (Wullschleger *et al.* 1991; Smillie *et al.* 1999; Gebbing and Schnyder 2001; Ruuska *et al.* 2004).

Acknowledgements

We thank Tiffany Barlow, Nicole Grant and Laura Howie for assistance in the field and with chlorophyll fluorescence analyses, Spencer Whitney (ANU) for generously providing Rubisco primary antibody, Jodie Dunn for assistance with HPLC, Shizue Matsubara for a lutein epoxide standard, and David Hollingworth for the photography and image layout in the supplementary figures.

References

Aschan G, Pfanz H (2003) Non-foliar photosynthesis - a strategy of additional carbon acquisition. *Flora* **198**, 81-97.

Aschan G, Pfanz H, Vodnik D, Batic F (2005) Photosynthetic performance of vegetative and reproductive structures of green hellebore (*Helleborus viridis* L. agg.). *Photosynthetica* **43**, 55-64.

Asokanthan PS, Johnson RW, Griffith M, Krol M (1997) The photosynthetic potential of canola embryos. *Physiologia Plantarum* **101**, 353-360.

Bazzaz FA, Carlson RW, Harper JL (1979) Contribution to reproductive effort by photosynthesis or flowers and fruits. *Nature* **270**, 554-555.

Biscoe PV, Gallagher JN, Littleton EJ, Monteith JL, Scott RK (1975) Barley and its environment: IV. Sources of assimilate for the grain. *Journal of Applied Ecology* **12**, 295-318.

Blanke MM, Lenz F (1989) Fruit photosynthesis. *Plant, Cell and Environment* **12**, 31-46.

Blanke MM, Notton BA, Hucklesby DP (1986) Physical and kinetic properties of photosynthetic phosphoenolpyruvate carboxylase in developing apple fruit. *Phytochemistry* **25**, 601-606.

Buchmann N, Kao W-Y, Ehleringer JR (1997) Influence of stand structure on carbon -13 of vegetation, soil, and canopy air within deciduous and evergreen forests in Utah, United States. *Oecologia* **110**, 109-119.

Bungard RA, Ruban AV, Hibberd JM, Press MC, Horton P, Scholes JD (1999) Unusual carotenoid composition and a new type of xanthophyll cycle in plants. *Proceedings of the National Academy of Sciences USA* **96**, 1135-1139.

Cipollini ML, Levey DJ (1991) Why some fruits are green when they are ripe: carbon balance in fleshy fruits. *Oecologia* **88**, 371-377.

Clément C, Mischler P, Burrus M, Audran J-C (1997) Characteristics of the photosynthetic apparatus and CO_2 fixation in the flower bud of *Lilium*. II. Anther. *International Journal Of Plant Sciences* **158**, 801-810.

Close DC, Davidson NJ, Davies NW (2006) Seasonal Fluctuations in pigment chemistry of co-occurring plant hemi-parasites of distinct form and function. *Environmental and Experimental Botany* **58**, 41-46.

Dunn JL, Turnbull JD, Robinson SA (2004) Comparison of solvent regimes for the extraction of photosynthetic pigments from the leaves of higher plants. *Functional Plant Biology* **31**, 195-202.

Duranceau M, Ghashghaie J, Brugnoli E (2001) Carbon isotope discrimination during photosynthesis and dark respiration in intact leaves of *Nicotiana sylvestris*: comparisons between wild type and mitochondrial mutant plants. *Australian Journal of Plant Physiology* **28**, 65-71.

Eastmond PJ, Rawsthorne S (1998) Comparison of the metabolic properties of plastids isolated from developing leaves or embryos of *Brassica napus* L. *Journal of Experimental Botany* **49**, 1105-1111.

Edelenbos M, Christensen LP, Grevsen K (2001) HPLC determination of chlorophyll and carotenoid pigments in processed green pea cultivars (*Pisum sativum* L.). *Journal of Agricultural and Food Chemistry* **49**, 4768-4774.

Esteban R, Jiménez ET, Jiménez MS, Morales D, Hormaetxe K, Becerril JM, García-Plazaola JI (2007) Dynamics of violaxanthin and lutein epoxide xanthophyll cycles in Lauraceae tree species under field conditions. *Tree Physiology* **27**, 1407-1414.

Esteban R, Jiménez MS, Morales D, Jiménez ET, Hormaetxe K, Becerril JM, Osmond CB, García-Plazaola JI (2008) Short- and long-term modulation of the lutein epoxide and violaxanthin cycles in two species of the Lauraceae: sweet bay laurel (*Laurus nobilis* L.) and avocado (*Persea americana* Mill.). *Plant Biology* **10**, 288-297.

Farquhar GD, Ehleringer JR, Hubick KT (1989) Carbon isotope discrimination and photosynthesis. *Annual Review of Plant Physiology and Plant Molecular Biology* **40**, 503-537.

Flinn AM, Pate JS (1970) A quantitative study of carbon transfer from pod and subtending leaf to the ripening seeds of the field pea (*Pisum arvense* L.). *Journal of Experimental Botany* **21**, 71-82.

Furbank RT, White R, Palta JA, Turner NC (2004) Internal recycling of respiratory CO2 in pods of chickpea (*Cicer arietinum* L.): the role of the pod wall, seed coat, and embryo. *Journal of Experimental Botany* **55**, 1687-1696.

García-Plazaola JI, Hernández A, Errasti E, Becerril JM (2002) Occurrence and operation of the lutein epoxide cycle in *Quercus* species. *Functional Plant Biology* **29**, 1075-1080.

García-Plazaola JI, Hernández A, Olano JM, Becerril JM (2003) The operation of the lutein epoxide cycle correlates with energy dissipation. *Functional Plant Biology* **30**, 319-324.

García-Plazaola JI, Hormaetxe K, Hernández A, Olano JM, Becerril JM (2004) The lutein epoxide cycle in vegetative buds of woody plants. *Functional Plant Biology* **31**, 815-823.

García-Plazaola JI, Matsubara S, Osmond CB (2007) The lutein epoxide cycle in higher plants: its relationships to other xanthophyll cycles and possible functions. *Functional Plant Biology* **34**, 759-773.

Gebbing T, Schnyder H (2001) ^{13}C Labelling kinetics of sucrose in glumes indicates significant refixation of respiratory CO_2 in the wheat ear. *Australian Journal of Plant Physiology* **28**, 1047-1053.

Gilmore AM, Yamamoto HY (1991) Resolution of lutein and zeaxanthin using a non-endcapped lightly carbon-loaded C_{18} high-performance liquid chromatographic column. *Journal of Chromatography* **543**, 137-145.

Goldstein G, Sharifi MR, Kohorn LU, Lighton JRB, Shultz L, Rundel PW (1991) Photosynthesis by inflated pods of a desert shrub, *Isomeris arborea*. *Oecologia* **85**, 396-402.

Grant NM, Miller RE, Watling JR, Robinson SA (2008) Synchronicity of thermogenic activity, alternative pathway respiratory flux, AOX protein content and carbohydrates in receptacle tissues of sacred lotus during floral development. *Journal of Experimental Botany* **59**, 705-714.

Griffiths H (1993) Carbon isotope discrimination. In 'Photosynthesis and production in a changing environment: a field and laboratory manual'. (Eds DO Hall, JMO Scurlock, HR Bolhàr-Nordenkampf, RC Leegood and SP Long). (Chapman and Hall: London)

Harvey DM, Hedley CL, Keely RJ (1976) Photosynthetic and respiratory studies during pod and seed development in *Pisum sativum* L. *Annals Of Botany* **40**, 993-1001.

Heaton THE, Crossley A (1995) Carbon isotope variations in a plantation of Sitka spruce, and the effect of acid mist. *Oecologia* **103**, 109-117.

Kevan PG (1983) Floral colors through the insect eye: What are they and what they mean. In 'Handbook of Experimental Pollination Biology'. (Eds CE Jones and RJ Little) pp. 3-30. (Van Nostrand Reinhold Company: New York)

Kirichenko EB, Krendeleva T, Koukariskikh G, Nizovskaia N (1993) Photochemical activity in chloroplasts of anthers and caryopsis pericarp in cereals. *Russian Journal of Plant Physiology* **40**, 229-233.

Kondo M, Muraoka H, Uchida M, Yazaki Y, Koizumi H (2005) Refixation of respired CO_2 by understory vegatation in a cool-temperate deciduous forest in Japan. *Agricultural and Forest Meteorology* **134**, 110-121.

Laemmli UK (1970) Cleavage of structural proteins during the assembly of the head of bacteriophage T4. *Nature* **227**, 680-685.

Lin G, Ehleringer JR (1997) Carbon isotopic fractionation does not occur during dark respiration in C_3 and C_4 plants. *Plant Physiology* **114**, 391-394.

Lüttge U, Fetene M, Liebig M, Rascher U, Beck E (2001) Ecophysiology of niche occupation by two giant rosette plants, *Lobelia gibberoa* Hemsl and *Solanecio gigas* (Vatke) C. Jeffrey, in an Aftromontane forest valley. *Annals of Botany* **88**, 267-278.

Matsubara S, Morosinotto T, Osmond CB, Bassi R (2007) Short- and long-term operation of the lutein-epoxide cycle in light-harvesting antenna complexes. *Plant Physiology* **144**, 926-941.

Matsubara S, Naumann M, Martin R, Nichol C, Rascher U, Morosinotto T, Bassi R, Osmond CB (2005) Slowly reversible de-epoxidation of lutein-epoxide in deep shade leaves of a tropical tree legume may "lock-in" lutein-based photoprotection during acclimation to strong light *Journal of Experimental Botany* **56**, 461-468.

Matus Z, Molnar P, Szabo LG (1993) Main carotenoids in pressed seeds (*Cucurbitae semen*) of oil pumpkin (*Cucurbita pepo* convar. *pepo* var. styriaca). *Acta Pharmaceutica Hungarica* **63**, 247-256.

Maxwell K, Johnson GN (2000) Chlorophyll flurorescence - a practical guide. *Journal of Experimental Botany* **51**.

Meeuse BJD (1975) Thermogenic respiration in aroids. *Annual Review of Plant Physiology* **26**, 117-126.

Merzlyak MN, Solovchenko AE (2002) Photostability of pigments in ripening apple fruit: a possible photoprotective role of carotenoids during plant senescence. *Plant Science* **163**, 881-888.

Peng C-L, Lin Z-F, Su Y-Z, Lin G-Z, Dou H-Y, Zhao C-X (2006) The antioxidative function of lutein: electron spin resonance studies and chemical detection. *Functional Plant Biology* **33**, 839-846.

Rabinowitch HD, Budowski P, Kedar N (1975) Carotenoids and epoxide cycles in mature-green tomatoes. *Planta* **122**, 91-97.

Razungles AJ, Babic I, Sapis J-C, Bayonove CL (1996) Particular behavior of epoxy xanthophylls during veraison and maturation of grape. *Journal of Agricultural and Food Chemistry* **44**, 3821-3825.

Robinson SA, Russell AW (1999) Development of the photosynthetic apparatus in Australian rainforest leaves. In 'Photosynthesis: Mechanisms and Effects'. (Ed. G Gareb) pp. 3991-3994. (Kluwer Academic Publishers: Dordrecht, The Netherlands)

Ruuska SA, Schwender J, Ohlrogge JB (2004) The capacity of green oilseeds to utilize photosynthesis to drive biosynthetic processes. *Plant Physiology* **136**, 2700-2709.

Salopek-Sondi B, Kovac M, Ljubesic N, Magnus V (2000) Fruit initiation in *Helleborus niger* L. triggers chloroplast formation and photosynthesis in the perianth. *Journal of Plant Physiology* **157**, 357-364.

Santoni V, Bellini C, Caboche M (1994) Use of two-dimensional protein-pattern analysis for the characterization of *Arabidopsis thaliana* mutants. *Planta* **192**, 557-566.

Schleser GH (1990) Investigations of the $\delta^{13}C$ pattern in leaves of *Fagus sylvatica* L. *Journal of Experimental Botany* **41**, 565-572.

Smillie RM, Hetherington SE, Davies WJ (1999) Photosynthetic activity of the calyx, green shoulder, pericarp, and locular parenchyma of tomato fruit. *Journal of Experimental Botany* **50**, 707-718.

Sternberg L, Moreira MZ, Martinelli LA, Victoria RL, Barbosa EM, Bonates LCM, Nepstad DC (1997) Carbon dioxide recycling in two Amazonian tropical forests. *Agricultural and Forest Meteorology* **88**, 259-268.

Tai C-Y, Chen BH (2000) Analysis and stability of carotenoids in the flowers of daylily (*Hemerocallis disticha*) as affected by various treatments. *Journal of Agricultural and Food Chemistry* **48**, 5962-5968.

Thayer SS, Björkman O (1990) Leaf xanthophyll content and composition in sun and shade determined by HPLC. *Photosynthesis Research* **23**.

Vemmos SN, Goldwin GK (1994) The photosynthetic activity of Cox's orange pippin apple flowers in relation to fruit setting. *Annals Of Botany* **73**, 385-391.

Watling JR, Robinson SA, Seymour RS (2006) Contribution of the alternative pathway to respiration during thermogenesis in flowers of the sacred lotus. *Plant Physiology* **140**, 1367-1373.

Watson TL, Close DC, Davidson NJ, Davies NW (2004) Pigment dynamics during cold-induced photoinhibition of *Acacia melanoxylon*. *Functional Plant Biology* **31**, 481-489.

Whitney SM, Andrews TJ (2001) Plastome-encoded bacterial ribulose-1,5-bisphosphate carboxylase oxygenase (RubisCO) supports photosynthesis and growth in tobacco. *Proceedings of the National Academy of Sciences U.S.A.* **98**, 14738-14743.

Wullschleger SD, Oosterhuis DM, Hurren RG, Hanson PJ (1991) Evidence for light-dependent recycling of respired carbon dioxide by the cotton fruit. *Plant Physiology* **97**, 574-579.

Tables

Table 1. Pigment composition (% of total carotenoid pool) in lotus receptacle stages and leaves.

Data are means ± 1 SE of *n*=5-8 and * indicates proportions in leaves that are significantly different to those in stage 5 receptacles at $P<0.05$.

Proportion (%)	Stage 0	Stage 1	Stage 2	Stage 3	Stage 4	Stage 5	Leaf
VAZ	34.1 ± 0.9	36.8 ± 0.9	37.8 ± 1.0	29.7 ± 1.1	36.7 ± 0.9	32.6 ± 0.8	22.8 ± 2.6*
Lutein	21.8 ± 1.6	29.6 ± 0.6	35.6 ± 0.4	37.1 ± 1.7	40.3 ± 1.7	45.9 ± 0.3	52.1 ± 1.9*
Lutein epoxide	32.3 ± 1.9	19.5 ± 1.9	8.5 ± 1.4	8.1 ± 1.3	3.9 ± 0.5	1.6 ± 0.2	0.5 ± 0.24*
β-carotene	1.6 ± 0.05	2.1 ± 0.1	1.5 ± 0.2	2.8 ± 0.5	4.7 ± 0.7	8.7 ± 0.25	10.9 ± 1.03
Neoxanthin	8.4 ± 0.3	7.4 ± 0.4	5.5 ± 0.4	4.4 ± 0.6	5.0 ± 0.6	9.4 ± 0.37	13.1 ± 0.70*

.

Table 2. Mean (± 1 SE) photosynthetic electron transport characteristics of lotus leaves, and of receptacles during greening.

Tissues which do not share the same superscript differ significantly at $P<0.05$ (Fv/Fm: $F_{3,29}=6.13$, $P=0.0027$; ETR: $F_{3,15}=56.6$, $P<0.0001$). * instantaneous ETR measured in the field, incident PFD was 1350 μmol m^{-2} s^{-1}.

Developmental Stage	Intrinsic quantum efficiency (Fv/Fm)	In situ ETR* (μmol m^{-2} s^{-1})
Stage 3 receptacle	0.53 ± 0.069^{a}	91.9 ± 6.2^{a}
Stage 4 receptacle	0.64 ± 0.037^{ab}	158.5 ± 8.8^{b}
Stage 5 receptacle	0.69 ± 0.013^{b}	201.6 ± 5.5^{c}
Leaf	0.76 ± 0.018^{b}	208.3 ± 8.7^{c}

Table 3. Mean $\delta^{13}C$ values of fully expanded sacred lotus leaves, and receptacles during development (greening).

Data are means ± 1 SE of *n*=5 samples. Tissues which do not share the same letter differ significantly ($F_{3,19}$=17.7, *P*<0.0001).

Developmental Stage	$\delta^{13}C$ (mean ± SD)
Leaf	-25.24 ± 0.15[a]
Stage 3 receptacle	-25.69 ± 0.21[ac]
Stage 4 receptacle	-26.42 ± 0.40[bc]
Stage 5 receptacle	-27.85 ± 0.27[d]

Figure Captions

Fig. 1. (a) Relative amounts of Rubisco (chemiluminescence output per g protein loaded per gel lane), (b) mean total chlorophyll (*a*+*b*), and (c) total carotenoid content in lotus leaves and the top surface layer (1 mm thick) of lotus receptacles throughout a developmental sequence. Data are means ± 1 SE of *n*=5-8 samples. Letters indicate significant differences (nmol g^{-1} FW) between receptacle developmental stages at $P<0.05$; significant differences between leaves and stage 5 receptacles are indicated by *. ND indicates no data.

Fig. 2. Mean pigment content (nmol g^{-1} FW) of sacred lotus receptacles throughout a developmental sequence: (a) lutein and lutein epoxide, (b) xanthophyll cycle pigments (VAZ), (c) neoxanthin, (d) β−carotene. Data are means ± 1 SE of *n*=5-8 samples. Significant differences at $P<0.05$ are indicated by the letters.

Fig. 3. Photosynthetic photon flux density (PFD) response curves of stage 3, 4 and 5 lotus receptacles: (a) relative electron transport rate (ETR), (b) effective quantum yield of photosystem II (ΦPSII), and (c) non-photochemical quenching (NPQ). Data are means ± 1 SE of *n*=6, 8, 8 for stages 3, 4 and 5, respectively.

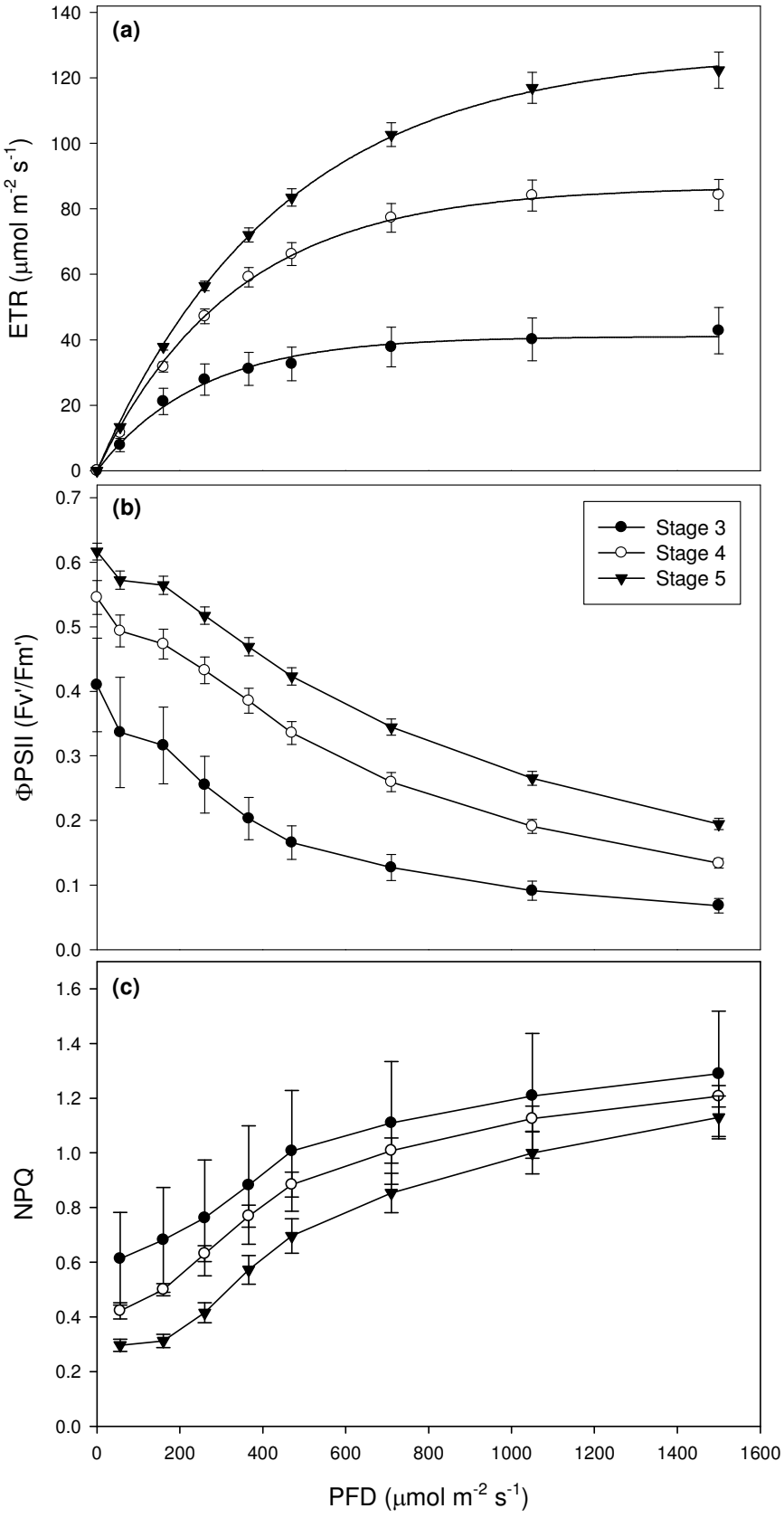
(a)
ETR (μmol m-2 s-1)
0
20
40
60
80
100
120
140
(b)
ΦPSII (Fv'/Fm')
0.0
0.1
0.2
0.3
0.4
0.5
0.6
0.7
Stage 3
Stage 4
Stage 5
(c)
NPQ
0.0
0.2
0.4
0.6
0.8
1.0
1.2
1.4
1.6
0
200
400
600
800
1000
1200
1400
1600
PFD (μmol m-2 s-1)

Figure 1

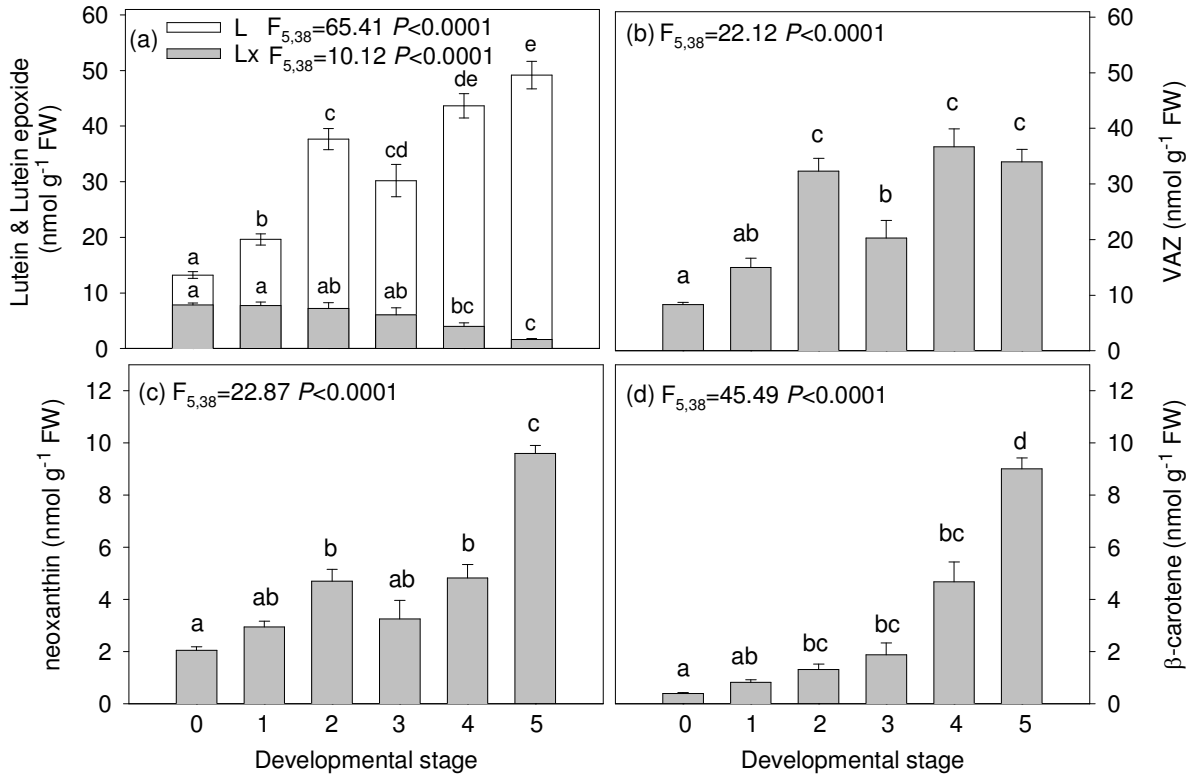
(a)
L $F_{5,38}$=65.41 P<0.0001
Lx $F_{5,38}$=10.12 P<0.0001
Lutein & Lutein epoxide (nmol g^{-1} FW)
(b) $F_{5,38}$=22.12 P<0.0001
VAZ (nmol g^{-1} FW)
(c) $F_{5,38}$=22.87 P<0.0001
neoxanthin (nmol g^{-1} FW)
(d) $F_{5,38}$=45.49 P<0.0001
β-carotene (nmol g^{-1} FW)
Developmental stage
Developmental stage

Figure 2

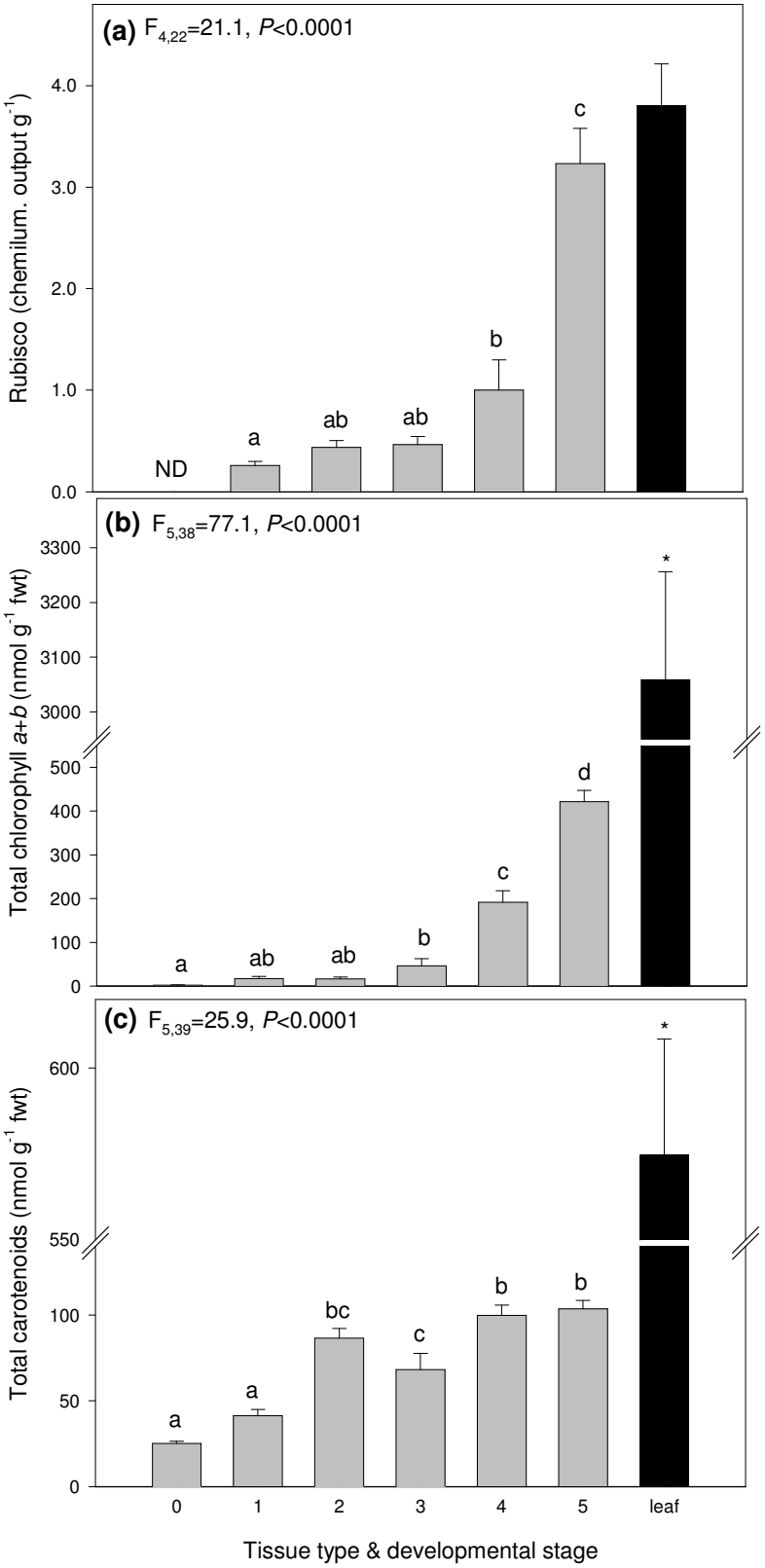
(a) $F_{4,22}$=21.1, P<0.0001
Rubisco (chemilum. output g^{-1})
4.0
3.0
2.0
1.0
0.0
ND
a
ab
ab
b
c
(b) $F_{5,38}$=77.1, P<0.0001
Total chlorophyll a+b (nmol g^{-1} fwt)
3300
3200
3100
3000
500
400
300
200
100
0
a
ab
ab
b
c
d
*
(c) $F_{5,39}$=25.9, P<0.0001
Total carotenoids (nmol g^{-1} fwt)
600
550
100
50
0
a
a
bc
c
b
b
*
0
1
2
3
4
5
leaf
Tissue type & developmental stage

Figure 3

Supplementary Fig. 1. Developmental stages of sacred lotus. Top panel L-R: Stage 0, small pre-thermogenic bud, enclosing small yellow receptacle; stage 1, larger bud, petals closed, yellow receptacle, onset of thermogenesis; stage 2, petals open between 2-12 cm, receptive stigmas, immature stamens appressed to yellow receptacle visible, peak thermogenesis. Bottom panel L-R: stage 3, petals horizontal, mature stamens falling away from receptacle, thermogenic activity subsides; stage 4, petals and stamens senesce and abscise, leaving postthermogenic yellow/green receptacle; and stage 5, larger green receptacle (8-12 cm diameter).

Supplementary Fig. 2. Sectioned green stage 5 receptacle showing the outer photosynthetic tissue layer, location of ovules and the spongy inner tissue. Scale bar is 1 cm.